

# Gradient Climbing in Formation via Extremum Seeking and Passivity-Based Coordination Rules

Emrah Biryik and Murat Arcak

Department of Electrical, Computer, and Systems Engineering

Rensselaer Polytechnic Institute, Troy, NY 12180

Emails: biyike@rpi.edu, arcakm@rpi.edu

**Abstract**—We consider a gradient climbing problem where the objective is to steer a group of vehicles to the extrema of an unknown scalar field distribution while keeping a prescribed formation. We address this task by developing a scheme in which the leader performs extremum seeking for the minima or maxima of the field, and other vehicles follow according to passivity-based coordination rules. The extremum-seeking approach generates approximate gradients of the field locally by “dithering” sensor positions. We show that if there is sufficient time-scale separation between the fast dither and slow gradient motions of the leader vehicle, the followers only respond to the gradient motion, and filter out the dither component, while keeping the prescribed formation.

## I. INTRODUCTION

Recent years have witnessed an increasing number of feedback applications in mobile sensor networks, cooperative robotics, and vehicle formations. For formation stability local feedback rules have been derived from artificial attraction and repulsion forces with neighboring vehicles [1], [2], [3]. The recent study [4] presented a unifying passivity framework for several group coordination problems, including formation design and group agreement. This passivity framework encompasses and broadens the Lyapunov analysis in several earlier results, including [1]. The references [1] and [4], however, assume that the reference velocity of the formation is available to each agent, and develop control laws that make use of this information. To remove this restriction, reference [5] addresses the case where the reference velocity information is available only to the leader, and develops an adaptive design that enables the other agents to reconstruct this information. In [5] the reference velocity is assigned to the leader *a priori*. In some applications, however, the vehicle may need to change the reference velocity while performing a certain task, *e.g.* source seeking [6], [7], or responding to an external stimulus, *e.g.* obstacle avoidance.

In this paper we allow the leader to autonomously change the reference velocity during the group motion, and study the effect of this change on the formation dynamics. In particular, we consider “gradient climbing” [2], [3], [8], [9] in which the leader performs extremum seeking for the field minima or maxima, and other vehicles follow according to passivity-based coordination rules. Keeping a group formation during the transients may be desirable for reliable inter-vehicle communication/sensing, drag reduction, safety in adversarial environments, etc. An example of a leader-following based formation design is presented in [10] where the followers carry a load cooperatively in a planetary terrain exploration mission.

Unlike the sensor coverage problem in [9] and the least-squares gradient estimation proposed in [2], [8], which rely on multiple sensor information, the extremum-seeking approach generates approximate gradients locally, by “dithering” sensor positions. The

advantage of this local approximation is that only designated leaders need sensing capabilities, and communication of sensed variables and geographic proximity of sensors are not necessary for generating approximate gradients. Indeed, it is noted in [11] that *E. coli* bacteria perform a similar dynamic sampling process to individually estimate gradients for foraging. Our leader-only sensing scheme is advantageous in applications where the sampling process is expensive, *e.g.* in monitoring contamination of sediments [12].

One of the mainstream approaches in extremum-seeking design is to probe the system with sinusoidal inputs, and to make an on-line estimation of the gradient of the output relative to these inputs [13]. An alternative approach relies on nonlinear optimization techniques to estimate the gradient information in discrete-time [14]. Earlier applications of extremum seeking to formation flight in [15], [16] aim to maximize the induced lift for the wingman, and do not address the search of a field distribution. Recent papers [6], [7] address source seeking of a single vehicle by employing continuous-time extremum seeking methods. The vehicle uses a sinusoidal perturbation to compute the gradient of the field and updates its velocity accordingly in continuous-time.

In this paper we take a discrete-time, optimization based extremum seeking approach. In our design, to achieve a successful gradient climbing by a group of vehicles while keeping a formation, the leader has a parameterized velocity that facilitates an adaptive reconstruction of this information by the followers. We show that if there is sufficient time-scale separation between the fast dither and slow gradient motions of the leader vehicle, the followers only respond to the gradient motion, and filter out the dither component.

The subsequent sections are organized as follows: Section II presents the extremum-seeking motion of the leader vehicle, and proves practical convergence to the maxima of the field. Section III reviews the passivity framework for group coordination developed in [4]. Section IV combines leader vehicle’s extremum seeking motion with the followers’ coordination laws, and proves the stability of the formation while locating the extrema of the field distribution. Section V gives a design example that illustrates the proposed scheme. Section VI concludes the paper.

## II. REFERENCE VELOCITY ASSIGNMENT VIA EXTREMUM SEEKING

In this section, we present the extremum seeking scheme performed by the leader. The detailed analysis of the motion of the group will be pursued in Section IV. Our goal in extremum-seeking based gradient climbing is to search for and move towards the maximum of a field distribution with an unknown functional form. We follow the optimization approach, where the vehicle has access only to the scalar field measurements, and constructs the approximate gradient and Hessian information of the field by finite-difference methods to compute a Newton direction. The motion

This work was supported in part by NSF under grant no. ECS-0238268 and by AFOSR under grant no. FA9550-07-1-0308.

controller on the vehicle then assigns the appropriate velocity that drives the vehicle along the computed Newton direction. It is important to note that, in this scheme, the vehicle locates the maxima without position measurements.

We first review the basic optimization tools that are instrumental in our extremum seeking design. We assume the field has a spatial distribution characterized by a twice continuously differentiable function<sup>1</sup>  $F(x) : \mathbb{R}^2 \rightarrow \mathbb{R}$  that has a unique<sup>2</sup> maximum at  $x = x^*$ . Because only field measurements are available to the leader, we employ one-sided finite-difference gradient,  $G_k$ ,

$$\nabla F(x_k) \approx G_k[i] := \frac{F(x_k + h_k e_i) - F(x_k)}{h_k} \quad (1)$$

and Hessian,  $H_k$ ,

$$\nabla^2 F(x_k) \approx H_k[i, j] := \frac{1}{h_k^2} \left[ F(x_k) + F(x_k + h_k e_i + h_k e_j) - F(x_k + h_k e_i) - F(x_k + h_k e_j) \right] \quad (2)$$

approximations, where  $h_k$  denotes the finite-difference “dither” size, and  $e_i$  is the  $i^{\text{th}}$  unit vector. Alternative methods such as line-search, Quasi-Newton (BFGS) [17], and Simultaneous Perturbation Stochastic Approximations (SPSA) [18], [19] are briefly discussed in Section VI. For an easier implementation, steepest descent (only three field measurements) may be preferable over Newton’s Method; however, it is slower and does not provide a concrete convergence proof with nonvanishing step-size. We denote by  $\mathcal{N}(\bar{x}, a)$  the ball of radius  $a$  centered at  $\bar{x}$ , i.e.  $\mathcal{N}(\bar{x}, a) := \{x : \|x - \bar{x}\| \leq a\}$ . The lemma below states that for sufficiently small dither size  $h_k$ , and for small initial error  $\|x_0 - x^*\|$ , finite-difference based Newton’s Method locally converges to an  $\mathcal{O}(h)$ -neighborhood of  $x^*$ . The proof follows from standard arguments in unconstrained optimization theory, and is omitted due to space restrictions.

**Lemma 1:** Let  $F(x) : \mathbb{R}^2 \rightarrow \mathbb{R}$  be twice continuously differentiable in an open convex set  $D \in \mathbb{R}^2$ . Assume there exists a unique  $x^* \in \mathbb{R}^2$ ,  $r > 0$  such that  $\mathcal{N}(x^*, r) \in D$ ,  $\nabla F(x^*) = 0$ ,  $\nabla^2 F(x^*)^{-1}$  exists with  $\|\nabla^2 F(x^*)^{-1}\| \leq \beta$ ,  $\nabla F(x)$  and  $\nabla^2 F(x)$  are Lipschitz continuous. Then there exist  $\epsilon > 0$  and  $\bar{h} > 0$ , such that for all initial conditions  $x_0 \in \mathcal{N}(x^*, \epsilon)$ , and dither size  $h_k < \bar{h}$  the sequence  $\{x_k\}_{k=0}^{\infty}$  generated by

$$x_{k+1} = x_k + H_k^{-1} G_k, \quad k = 0, 1, \dots \quad (3)$$

where  $G_k$  and  $H_k$  are as in (1)-(2) converges to an  $\mathcal{O}(\bar{h})$  neighborhood of  $x^*$   $q$ -linearly. ■

We next introduce the Newton’s Method-based extremum seeking scheme that the leader performs to locate the maximum of the field. Following the passivity framework introduced in [4], we consider agents with the dynamic model

$$\dot{x}_i = h_i(\xi_i, u_i) + v(t), \quad i = 1, \dots, N \quad (4)$$

$$\dot{\xi}_i = f_i(\xi_i, u_i) \quad (5)$$

where  $x_i \in \mathbb{R}^2$  and  $\xi \in \mathbb{R}^2$  denote the position and internal dynamics of each vehicle, respectively,  $u_i$  is an external feedback law to be designed later in (23), and  $v(t)$  is the reference group velocity. An example of such a model is the fully-actuated point mass

$$\ddot{x}_i = f_i \quad (6)$$

<sup>1</sup>We restrict our attention to  $\mathbb{R}^2$ , however, our results can be extended to  $\mathbb{R}^3$  as well by employing appropriate finite-difference approximations.

<sup>2</sup>If the function  $F(x)$  has multiple maxima, then our results can be modified to prove regional convergence to the local maximum.

where  $x_i \in \mathbb{R}^2$  is the position of each mass and  $f_i \in \mathbb{R}^2$  is the input force. Indeed, the internal feedback law

$$f_i = -K_i(\dot{x}_i(t) - v(t)) + \dot{v}(t) + u_i, \quad K_i > 0 \quad (7)$$

and the change of variables  $\xi_i = \dot{x}_i - v(t)$  bring (6) into the form

$$\dot{x}_i = \xi_i + v(t) \quad (8)$$

$$\dot{\xi}_i = -K_i \xi_i + u_i \quad (9)$$

which is as in (4)-(5). The leader, say the first vehicle, does not receive external feedback from other members of the group, hence  $u_1 = 0$ . Without loss of generality we assume  $\xi_1(0) = 0$ , i.e. the vehicle is initially at rest, which yields the leader dynamics

$$\dot{x} = v_1(t). \quad (10)$$

Note that if  $\xi_1(0) \neq 0$ , we can apply the velocity input  $\tilde{v} = -h(\xi_1, 0) + v_1(t)$ , and recover (10).

We use Newton’s Method to determine the next position for the vehicle, and set the velocity  $v_1(t)$  to steer the vehicle to that position. In the  $k$ th extremum-seeking iteration, the leader first moves in  $[1, 0]$ ,  $[-1, 1]$ , and  $[0, -1]$  directions rapidly to take samples of the field  $F(x)$ , and computes the approximate gradient  $G_k$  and the Hessian  $H_k$  as in (1)-(2), and then moves in the approximate Newton direction  $d_k = H_k^{-1} G_k$ , and arrives at  $x_{k+1} = x_k + d_k$  as illustrated in Figure 1.

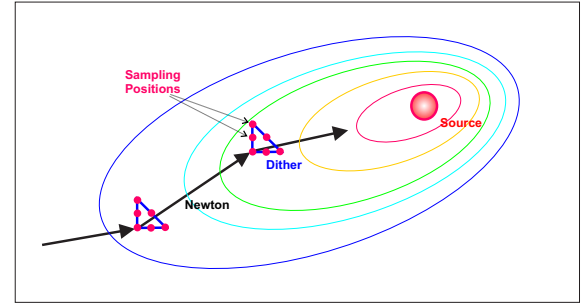


Fig. 1. Gradient climbing by extremum seeking. Arrows represent the slow Newton motion, while triangular paths represent the fast dither motion with the samples taken at positions marked by dots.

To prepare for an adaptive velocity estimation by the followers as in [5], we need to have the velocity vector in a parameterized form. For each motion segment we let the velocity have a fixed sinusoidal amplitude profile, with endpoints at zero, and change its direction between successive segments. This sinusoidal amplitude profile allows us to construct the velocity information of the vehicle adaptively using the results in [5]. There are other techniques to assign the velocity vector in discrete-time extremum seeking, e.g. set-point stabilization, [20], [21], but they require position measurements, and do not provide a parameterized reference velocity, hence are not suitable for the adaptive estimation design in this paper.

We let  $v_{[i,j]}$  and  $v_N$  denote the dither velocity in  $[i, j]$  direction,  $[i, j] \in \{[1, 0], [-1, 1], [0, -1]\}$ , and the Newton velocity in  $d_k$  direction, respectively, and  $\tau$  denote the duration of each dither motion segment, and  $T$  be that of the Newton motion. Therefore one iteration of the extremum seeking scheme takes  $\Delta := 3\tau + T$  seconds. During each extremum seeking iteration, the vehicle switches its velocity as

$$\dot{x}_1 = v_1(t) := \begin{cases} v_{[1,0]}(t), & \text{if } t_k \leq t < t_k + \tau, \\ v_{[-1,1]}(t), & \text{if } t_k + \tau \leq t < t_k + 2\tau, \\ v_{[0,-1]}(t), & \text{if } t_k + 2\tau \leq t < t_k + 3\tau, \\ v_N(t), & \text{if } t_k + 3\tau \leq t < t_{k+1}, \end{cases} \quad (11)$$

where  $t_k := k\Delta$ ,  $k = 0, 1, 2, \dots$ , and  $v_{[1,0]}$ ,  $v_{[-1,1]}$ ,  $v_{[0,-1]}$  and  $v_N$  are defined as in (12)-(15):

$$v_{[1,0]}(t) := \frac{2h_k}{\tau} \begin{matrix} 1 \\ 0 \end{matrix} \begin{matrix} 1 - \cos(\frac{2\pi}{\tau}(t - t_k)) \end{matrix} \quad (12)$$

$$v_{[-1,1]}(t) := \frac{2h_k}{\tau} \begin{matrix} -1 \\ 1 \end{matrix} \begin{matrix} 1 - \cos(\frac{2\pi}{\tau}(t - t_k - \tau)) \end{matrix} \quad (13)$$

$$v_{[0,-1]}(t) := \frac{2h_k}{\tau} \begin{matrix} 0 \\ -1 \end{matrix} \begin{matrix} 1 - \cos(\frac{2\pi}{\tau}(t - t_k - 2\tau)) \end{matrix} \quad (14)$$

$$v_N(t) := \frac{d_k}{T} \begin{matrix} 1 \\ 0 \end{matrix} \begin{matrix} 1 - \cos(\frac{2\pi}{T}(t - t_k - 3\tau)) \end{matrix} . \quad (15)$$

We note that the velocity input  $v_1(t)$  in (11) and its derivative  $\dot{v}_1(t)$  are continuous, and  $(v_1(t), \dot{v}_1(t))|_{t \in \{t_k + n\tau, t_{k+1}\}} = (0, 0)$ ,  $n = 0, 1, 2, 3$ . In our design, however, the choice of velocity profiles are not restricted to (12)-(15). Other continuous velocity profiles that vanish at  $t \in \{t_k + n\tau, t_{k+1}\}$ ,  $n = 0, 1, 2, 3$ , along with their derivatives, are also applicable. The velocities in (12)-(15), when switched according to (11), achieve one iteration of extremum-seeking motion by driving the vehicle first to the appropriate dither positions and then to the next “Newton” position  $x_{k+1}$ . Theorem 1 below proves that our extremum seeking scheme converges to an  $\mathcal{O}(\bar{h})$  neighborhood of the maximum  $x^*$ , when  $h_k \leq \bar{h}$  is as in Lemma 1, and  $\|x(0) - x^*\|$  is sufficiently small.

**Theorem 1:** *Let the field distribution  $F(x)$  be twice continuously differentiable with a unique maximum at position  $x = x^* \in \mathbb{R}^2$ . Suppose the assumptions in Lemma 1 hold and  $\bar{h}$  be as defined therein. Then the Newton-based extremum seeking scheme applied to the vehicle model in (11) with velocity profiles (12)-(15) drives the vehicle to the  $\mathcal{O}(\bar{h})$  neighborhood of  $x^*$ , provided that  $h_k \leq \bar{h}$  and  $\|x(0) - x^*\|$  is sufficiently small.* ■

**Proof of Theorem 1:** We show that the velocity profiles given in (11) first drive the vehicle in the appropriate dither directions, and then along the Newton direction. Consider  $v_{[1,0]}$  which drives the vehicle in horizontal position, i.e. along the vector  $[1, 0]$ . At time  $t_k$ , let the position of vehicle be  $x_k$ , then at time  $t_k + \tau/2$  its position is:

$$\begin{aligned} x(t_k + \frac{\tau}{2}) &= x(t_k) + \int_{t_k}^{t_k + \tau/2} v_{[1,0]}(t) dt \\ &= x(t_k) + \frac{2h_k}{\tau} \begin{matrix} 1 \\ 0 \end{matrix} \int_{t_k}^{t_k + \tau/2} (1 - \cos(\frac{2\pi}{\tau}(t - t_k))) dt \\ &= x(t_k) + \frac{2h_k}{\tau} \begin{matrix} 1 \\ 0 \end{matrix} \left[ t - \frac{\tau}{2\pi} \sin(\frac{2\pi}{\tau}(t - t_k)) \right]_{t_k}^{t_k + \tau/2} \\ &= x(t_k) + h_k \begin{matrix} 1 \\ 0 \end{matrix} = \begin{matrix} x^1(t_k) + h_k \\ x^2(t_k) \end{matrix} . \end{aligned} \quad (16)$$

Likewise,

$$\begin{aligned} x(t_k + \tau) &= x(t_k + \tau/2) + \int_{t_k + \tau/2}^{t_k + \tau} v_{[1,0]}(t) dt \\ &= x(t_k + \tau/2) + h_k \begin{matrix} 1 \\ 0 \end{matrix} = \begin{matrix} x^1(t_k) + 2h_k \\ x^2(t_k) \end{matrix} . \end{aligned} \quad (17)$$

Similar calculations show that  $v_{[-1,1]}$  and  $v_{[0,-1]}$  achieve the desired dither motions as well. Note that after the third dither motion  $v_{[0,-1]}$  the vehicle will be back at position  $x(t_k + 3\tau) = x(t_k) = x_k$ . Then, applying the velocity  $v_N$  after this point for  $T$  seconds drives the vehicle to

$$\begin{aligned} x(t_k + \Delta) &= x(t_k) + d_k \frac{1}{T} \int_{t_k + 3\tau}^{t_k + 3\tau + T} (1 - \cos(\frac{2\pi}{T}(t - t_k - 3\tau))) dt \\ &= x(t_k) + d_k = x(t_{k+1}). \end{aligned} \quad (18)$$

Therefore, by appropriately switching the velocities defined in (11) the vehicle visits all dither positions and then moves to the next Newton position. The convergence result follows from Lemma 1. ■

### III. REVIEW OF THE PASSIVITY FRAMEWORK FOR GROUP COORDINATION

We have shown that using the switching strategy in (11) with the velocity  $v_1(t)$  parameterized as in (12)-(15), the leader locates the extrema of the field. We next study the motion of the group while achieving the gradient climbing. We first review the passivity framework for group coordination [4], and adaptive reference velocity estimation of the followers [5]. Reference [4] studies a group of  $N$  agents, where each agent  $i = 1, \dots, N$  is represented by a vector  $x_i \in \mathbb{R}^p$  which is to be coordinated with the rest of the group. The communication structure between the agents is described by a graph. If the  $i$ th and  $j$ th agents have access to the relative information  $x_i - x_j$ , then the nodes  $i$  and  $j$  are connected by a link. Denoting by  $M$  the total number of links, we recall from [22] that the  $N \times M$  incidence matrix  $D$  of the graph is defined as

$$d_{ik} := \begin{cases} +1 & \text{if } i\text{th node is the positive end of the } k\text{th link} \\ -1 & \text{if } j\text{th node is the positive end of the } k\text{th link} \\ 0 & \text{otherwise.} \end{cases} \quad (19)$$

Reference [4] designs coordination laws that achieve the following objectives :

**B1)** Each member achieves in the limit a common velocity vector  $v(t) \in \mathbb{R}^p$  prescribed for the group; that is  $\lim_{t \rightarrow \infty} |\dot{x}_i - v(t)| = 0$ ,  $i = 1, \dots, N$ .

**B2)** If  $i$ th and  $j$ th members are connected by link  $k$ , then the difference variable  $z_k$

$$z_k := \sum_{l=1}^N d_{lk} x_l = \begin{cases} x_i - x_j, & \text{if } i \text{ is the positive end of } k\text{th link} \\ x_j - x_i, & \text{if } j \text{ is the positive end of } k\text{th link} \end{cases} \quad (20)$$

converges to a prescribed compact set  $\mathcal{A}_k \subset \mathbb{R}^p$ ,  $k = 1, \dots, M$ .

Examples of such target sets  $\mathcal{A}_k$  include the origin if  $x_i$ 's are variables that must reach an agreement within the group, or a sphere in  $\mathbb{R}^p$  if  $x_i$ 's are positions of vehicles that must maintain a prescribed distance.

Reference [4] assumes that, upon a change of variables and a preliminary feedback design, the agent dynamics can be brought into the form (4)-(5) where  $f_i(\cdot, \cdot)$  and  $h_i(\cdot, \cdot)$  are  $C^1$  functions such that  $h_i(0, 0) = 0$  and

$$f_i(0, u_i) = 0 \Rightarrow u_i = 0. \quad (21)$$

The main restriction in [4] is that the  $\xi_i$  subsystems in (5) be strictly passive with  $C^1$ , positive definite, radially unbounded storage functions  $S_i(\xi_i)$  satisfying

$$\dot{S}_i \leq -W_i(\xi_i) + u_i^T y_i \quad i = 1, \dots, N \quad (22)$$

for some positive definite functions  $W_i(\cdot)$ .

To achieve objectives B1 and B2, [4] proposes a class of feedback laws of the form

$$u_i = - \sum_{k=1}^M d_{ik} \psi_k(z_k) \quad (23)$$

in which the nonlinearities  $\psi_k(z_k)$  are of the form

$$\psi_k(z_k) = \nabla P_k(z_k) \quad (24)$$

where  $P_k(z_k)$  is a nonnegative  $C^2$  function

$$P_k : \mathcal{G}_k \rightarrow \mathbb{R}_{\geq 0} \quad (25)$$

defined on an open set  $\mathcal{G}_k \subseteq \mathbb{R}^p$ . If  $x_i$ 's are positions of vehicles that must maintain a prescribed distance, then the choice  $\mathcal{G}_k = \{x_i | x_i \in \mathbb{R}^p \setminus \{0\}\}$  disallows the possibility of collisions. To steer  $z_k$ 's into the target sets  $\mathcal{A}_k$ , we let  $P_k(z_k)$  and its gradient  $\nabla P_k(z_k)$  vanish on  $\mathcal{A}_k$ , let  $P_k(z_k)$  grow unbounded as  $z_k$  goes to the boundary of  $\mathcal{G}_k$ :

$$P_k(z_k) \rightarrow \infty \quad \text{as } z_k \rightarrow \partial \mathcal{G}_k \quad (26)$$

$$P_k(z_k) = 0 \Leftrightarrow z_k \in \mathcal{A}_k \quad (27)$$

$$\nabla P_k(z_k) = 0 \Leftrightarrow z_k \in \mathcal{A}_k. \quad (28)$$

To state the main result from [4] we introduce the concatenated vectors

$$x := [x_1^T, \dots, x_N^T]^T \quad z := [z_1^T, \dots, z_M^T]^T \quad (29)$$

$$u := [u_1^T, \dots, u_N^T]^T \quad \psi := [\psi_1^T, \dots, \psi_M^T]^T \quad (30)$$

and note from (20) and (23) that

$$z = (D^T \otimes I_p)x \quad (31)$$

$$u = -(D \otimes I_p)\psi(z) \quad (32)$$

where  $\otimes$  represents the Kronecker product and  $I_p$  denotes the  $p \times p$  identity matrix. Theorem 2 below, proven in [4], shows convergence of all trajectories to the set of equilibria

$$\mathcal{E} = \left\{ (z, \xi) \mid \xi = 0, (D \otimes I_p)\psi(z) = 0 \text{ and } z \in \mathcal{R}(D^T \otimes I_p) \right\}. \quad (33)$$

**Theorem 2:** Consider the coordination laws (4), (5) and (23) where  $v(t)$  is uniformly bounded and piecewise continuous and  $\mathcal{H}_i$ ,  $i = 1, \dots, N$ , and  $\psi(k)$ ,  $k = 1, \dots, M$  are designed as in (5), (21)-(22) and (24)-(28) for given open sets  $\mathcal{G}_k \subseteq \mathbb{R}^p$  and compact subsets  $\mathcal{A}_k \subset \mathcal{G}_k$ . Then, all trajectories  $(z(t), \xi(t))$  starting in  $\mathcal{G}$  converge to the set of equilibria  $\mathcal{E}$  in (33). ■

#### Leader Following: Adaptive Velocity Estimation

In the recent paper [5], the case where only the leader has the velocity information is studied, and an adaptive velocity estimation scheme that reconstructs this information is developed. Reference [5] assumes that the velocity of the leader  $v_1(t) \in \mathbb{R}^p$  is parameterized as

$$v_1(t) = \sum_{j=1}^r \phi^j(t) \theta^j$$

where  $\phi^j(t)$  are uniformly bounded scalar base functions available to each agent and  $\theta^j$  are column vectors available only to the leader. Other vehicles estimate the unknown  $\theta^j$  by  $\hat{\theta}^j$ , and construct reference velocity estimate  $\hat{v}_i(t)$  through the formula

$$\hat{v}_i(t) = \sum_{j=1}^r \phi^j(t) \hat{\theta}^j = (\Phi(t)^T \otimes I_p) \hat{\theta}_i \quad i = 2, \dots, N, \quad (34)$$

where  $\Phi(t) := [\phi^1(t), \dots, \phi^r(t)]^T$  and  $\hat{\theta}_i := [(\hat{\theta}_i^1)^T, \dots, (\hat{\theta}_i^r)^T]^T$ , and the parameter  $\hat{\theta}^j$  is obtained by the update law

$$\dot{\hat{\theta}}_i = \Lambda_i (\Phi(t) \otimes I_p) u_i \quad (35)$$

in which  $\Lambda_i = \Lambda_i^T > 0$  is the adaptive gain matrix and  $u_i$  is as in (23). It is proven in [5] that the convergence result in Theorem 2 is recovered by modifying (4) as

$$\dot{x}_1 = h_1(\xi_1, 0) + v_1(t) \quad (36)$$

$$\dot{x}_i = h_i(\xi_i, u_i) + \hat{v}_i(t) \quad i = 2, \dots, N. \quad (37)$$

#### IV. GRADIENT CLIMBING IN FORMATION

We now study the behavior of the group in response to the leader's extremum seeking motion. We combine the passivity-based group coordination laws with the leader's extremum seeking motion, and study the formation dynamics with respect to the leader's dynamics. Note that the followers do not have the knowledge of the velocity  $v_1(t)$  which changes after each iteration of extremum seeking. Our adaptive design aims to estimate the gradient motion component of  $v_1(t)$  while filtering out the fast dither motion component, so that the followers do not respond to the dither.

During the dither motion, the followers can turn off the velocity adaptation scheme so that they do not respond to the dither. Even if the adaptation is not turned off, an averaging analysis in [23, Section 10.6] shows that when  $\tau$  is small the followers detect only the slow Newton motion, and average out the dither component. Indeed, from (11), the average of the leader's dynamics within one extremum seeking iteration are

$$v_{1,av} := \frac{1}{\Delta} \int_{t_k}^{t_k+\Delta} v_1(t) dt = \frac{1}{\Delta} d_k, \quad (38)$$

and  $\Delta \approx T$  if  $\tau$  is small. Then, it follows from [5, Theorem 2] that using the adaptation law in (34), (35), (37) the formation is reconstructed within each extremum-seeking iteration if  $T$  is sufficiently large.

#### Two-Time-Scale Behavior During the Newton Motion

We now reveal the two-time-scale behavior in the group motion induced by a large  $T$ , and show that the convergence to the desired formation is achieved in the fast time scale, while the Newton motion is performed in the slow time-scale. We consider only the Newton motion segment of the group in  $k$ th extremum seeking iteration, and let  $w := 1/T$ ,  $\bar{t} := t - t_k - 3\tau$ ,  $\bar{t} \in [0, T]$ . Then in the slow time-scale  $\sigma := w\bar{t}$ , the leader dynamics in (10) become

$$\frac{dx_1}{d\sigma} = d_k \phi(\sigma), \quad \sigma \in [0, 1]. \quad (39)$$

where  $\phi(\sigma) := (1 - \cos(2\pi\sigma))$ . We let the base function available to the followers be  $\Phi(\sigma) := w\phi(\sigma) = w(1 - \cos(2\pi\sigma)) \in \mathbb{R}$  from (15), and assume a uniform adaptation gain  $\Lambda_i = \lambda I_2$ ,  $i = 2, \dots, N$ , in (35) where  $\lambda > 0$  is constant. We then denote by  $\tilde{\theta}_i$  the error variable

$$\tilde{\theta}_i = \hat{\theta}_i - \theta \quad i = 2, \dots, N$$

and note from (35) that

$$\dot{\tilde{\theta}}_i = \lambda \Phi(\sigma) u_i \quad i = 2, \dots, N \quad (40)$$

For consistency with (29) and (30), we set  $\tilde{\theta}_1 \equiv (0, 0)^T$ , and define

$$\tilde{\theta} = [\tilde{\theta}_1^T, \tilde{\theta}_2^T, \dots, \tilde{\theta}_N^T]^T.$$

Using (5), (31), (35), and the property

$$(D^T \otimes I_p)(1_N \otimes v(t)) = 0 \quad (41)$$

which results from the fact that the sum of the rows of  $D$  is zero, the fast  $(z, \xi, \tilde{\theta})$  dynamics are obtained as:

$$w \frac{dz}{d\sigma} = (D^T \otimes I_2)(h(\xi, u) + w\phi(\sigma)\tilde{\theta}), \quad (42)$$

$$w \frac{d\xi}{d\sigma} = f(\xi, u) + (D \otimes I_2)\psi(z), \quad (43)$$

$$\frac{1}{\lambda} \frac{d\tilde{\theta}}{d\sigma} = \phi(\sigma)(D \otimes I_2)\psi(z). \quad (44)$$



Note that  $w$  acts also as a regular perturbation parameter in  $z$ -dynamics. When  $w$  is small, the reference velocity is slowly time-varying, hence the mismatch between  $v_1(t)$  and  $\hat{v}(t)$  become less effective on the formation dynamics. We pick the adaptation gain  $\lambda = \mathcal{O}(T) = \mathcal{O}(1/w)$ , so that  $\hat{\theta}$  has fast dynamics as well. System (39), (42)-(44) is then in a singularly perturbed form. Letting  $w \rightarrow 0$  yields the quasi-steady state equations:

$$0 = (D^T \otimes I_2)h(\bar{\xi}, u), \quad (45)$$

$$0 = f(\bar{\xi}, u) + (D \otimes I_2)\psi(\bar{z}), \quad (46)$$

$$0 = \phi(\sigma)(D \otimes I_2)\psi(\bar{z}). \quad (47)$$

We note that (47) is time-varying, and average  $\phi(\sigma)$  over  $\sigma \in [0, 1]$  to obtain

$$0 = \int_0^1 \phi(\sigma) d\sigma (D \otimes I_2)\psi(\bar{z}) \quad (48)$$

$$= \int_0^1 (1 - \cos(2\pi\sigma)) d\sigma (D \otimes I_2)\psi(\bar{z}) \quad (49)$$

$$= (D \otimes I_2)\psi(\bar{z}) \quad (50)$$

which implies  $\bar{z}_k \in \mathcal{A}_k$ , and  $u = 0$  from (32). We then conclude  $f(\bar{\xi}, u) = 0$  from (46), which implies  $\bar{\xi} = 0$  from  $u = 0$  and (21), and satisfies (45). Then the quasi-steady states are  $(\bar{z}, \bar{\xi}) = (\bar{z}_k \in \mathcal{A}_k, 0)$ .

#### Rescaling the Formation Dynamics

Smaller  $T$  allows faster convergence to the field maxima, but it reduces the time-scale separation between leader motion and the rest of the dynamics. We now circumvent this trade-off by rescaling the design parameters, and accelerating the formation dynamics uniformly. We consider the model in (8)-(9), which yields

$$\dot{z} = (D^T \otimes I_2)\xi + w\phi(t)(D^T \otimes I_2)\tilde{\theta} \quad (51)$$

$$\dot{\xi} = -K\xi + (D \otimes I_2)\psi(z) \quad (52)$$

$$\dot{\tilde{\theta}} = \lambda w\phi(t)(D \otimes I_2)\psi(z), \quad (53)$$

where  $K = K^T := \text{diag}(K_i) > 0$ . When  $T$  is reduced to  $\epsilon T$ ,  $\epsilon < 1$ , we define the new variable  $\hat{\xi} := \epsilon\xi$  and rescale  $K$ ,  $\psi(\cdot)$  and  $\lambda$  as  $K \rightarrow K/\epsilon$ ,  $\psi(\cdot) \rightarrow \psi(\cdot)/\epsilon^2$ ,  $\lambda \rightarrow \epsilon^2\lambda$ . Then, in the new variables the system (51)-(53) takes the form

$$\epsilon\dot{z} = (D^T \otimes I_2)\hat{\xi} + w\phi(t)(D^T \otimes I_2)\tilde{\theta} \quad (54)$$

$$\epsilon\dot{\hat{\xi}} = -K\hat{\xi} + (D \otimes I_2)\psi(z) \quad (55)$$

$$\epsilon\dot{\tilde{\theta}} = \lambda w\phi(t)(D \otimes I_2)\psi(z), \quad (56)$$

which evolves in a faster time-scale than (51)-(53).

#### V. DESIGN EXAMPLE

We study the gradient climbing of four vehicles, modelled as fully-actuated point-masses

$$\ddot{x}_i = f_i, \quad i = 1, 2, 3, 4 \quad (57)$$

where  $x_i \in \mathbb{R}^2$  is the position of each mass and  $f_i \in \mathbb{R}^2$  is the input force.

To stabilize a rhombus formation with the relative distances  $|z_1| = |x_1 - x_2| = \sqrt{3}$ , and  $|z_k| = |x_i - x_j| = 1$ ,  $k = 2, \dots, 6$ ,  $i, j = 1, \dots, 4$ ,  $i \neq j$ , we design  $\mathcal{A}_1$  to be a circle with radius  $r = \sqrt{3}$ ,  $\mathcal{A}_k$  to be the unit circle,  $k = 2, \dots, 6$ ,  $\mathcal{G}_k$  to be  $\mathbb{R}^2 \setminus \{0\}$ , and let the potential functions be of the form

$$P_1(z_1) = \int_{\sqrt{3}}^{|z_1|} \sigma_1(s) ds, \quad P_k(z_k) = \int_1^{|z_k|} \sigma_k(s) ds \quad (58)$$

where  $\sigma_k : \mathbb{R}_{>0} \rightarrow \mathbb{R}$  is a  $C^1$ , strictly increasing function such that

$$\sigma_1(\sqrt{3}) = 0, \sigma_k(1) = 0, \lim_{s \rightarrow \infty} \sigma_k(s) = \infty, \lim_{s \rightarrow 0} \sigma_k(s) = -\infty \quad (59)$$

and such that, as  $|z_k| \rightarrow \infty$ ,  $P_k(z_k) \rightarrow \infty$  in (58). Then  $P_k(z_k)$  satisfies (24)-(28), and the feedback law (23) with the interaction forces

$$\psi_k(z_k) = \nabla P_k(z_k) = \sigma_k(|z_k|) \frac{1}{|z_k|} z_k \quad z_k \neq 0 \quad (60)$$

guarantees asymptotic stability of the desired formation from Theorem 2. For the simulations we take  $\sigma_1(s) = \ln(s/\sqrt{3})$  and  $\sigma_k(s) = \ln(s)$ .

We let the field distribution be

$$F(x, y) = e^{-0.1e^{0.1x}(1.1x-5)^2 - 0.2e^{0.1y}(0.8y-4)^2},$$

which has a global maximum at  $x = [4.5, 5]$ . We fix  $\Delta = 20$  and  $h_k = 0.05$ , and pick  $\tau = 0.5\text{sec}$  and  $T = 18.5\text{sec}$  for the first simulation. We run the system (36)-(37), where the leader determines its velocity by extremum seeking as in (11) and (12)-(15). Figure 2 shows that after an initial transient, vehicles follow the leader's Newton motion in a rhombus formation, and average out the fast dither perturbations, while the leader locates the maxima of the field. In the second simulation, we perform the dither motion at a slower speed with  $\tau = 4\text{sec}$ ,  $T = 8\text{sec}$ . In this case, the vehicles in Figure 3 fail to average out the dither motion, and follow a jittering trajectory.

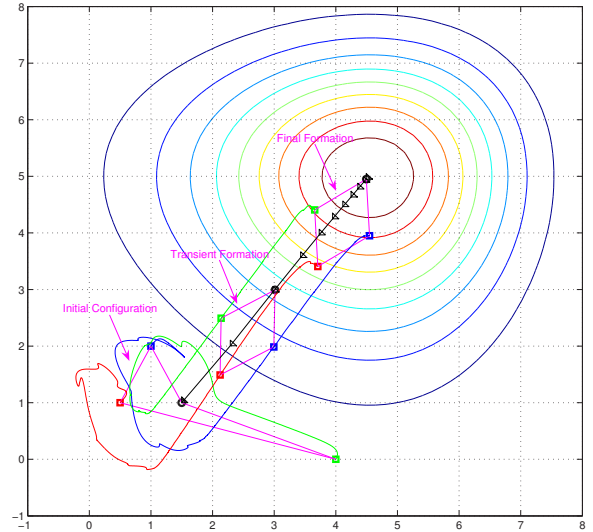


Fig. 2. Gradient climbing by Newton-based extremum seeking.  $T = 18.5$ ,  $\tau = 0.5$ ,  $h_k = 0.05$ . Black line represents the leader's trajectory, while red, blue, and green are the followers'. After an initial transient vehicles follow the leader's Newton motion in a rhombus formation, and average out the fast dither perturbations.

#### VI. DISCUSSION AND CONCLUSION

We considered a combined gradient climbing and formation design, and showed that if there is sufficient time-scale separation between the slow gradient motion and the fast dither motion, the formation dynamics act as a boundary-layer system relative to the leader vehicle dynamics. The leader's velocity is introduced in a parameterized form so that an adaptive reconstruction can be pursued by the rest of the vehicles to follow the gradient motion while averaging out dither motion.

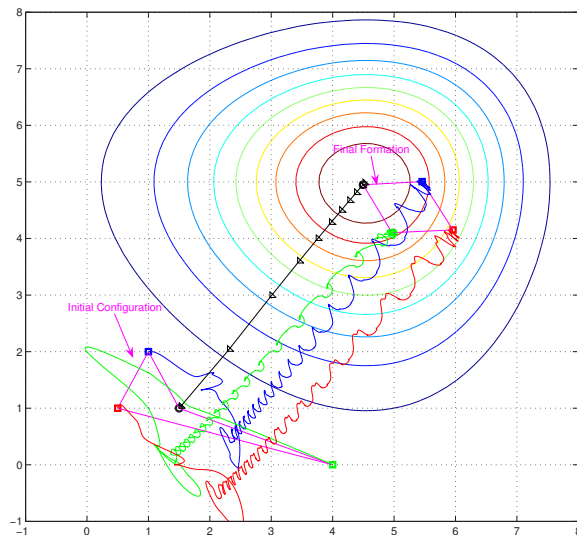


Fig. 3. Gradient climbing by Newton-based extremum seeking.  $T = 8$ ,  $\tau = 4$ ,  $h_k = 0.05$ . Black line represents the leader's trajectory, while red, blue, and green are the followers'. The vehicles fail to average out the dither motion, and follow a jittering trajectory.

Our Newton's Method based extremum seeking scheme proves local convergence to the maxima. Most of the global convergence results in the literature require a line search that adaptively finds a step size for each iteration. In a line search, however, additional function evaluations (field measurements) are required, which limits the applicability to our problem. The Quasi-Newton method BFGS recursively updates the Hessian approximation and, hence, reduces the number of measurements. A local *practical* convergence proof for BFGS can be pursued using the tools in [24] which rely on the exact knowledge of  $\nabla F(x)$ , and global versions can be achieved via line search. To address the effect of noise in the field and in the measurements, stochastic gradient approximations can be pursued, such as those in [25], [26]. To minimize the energy consumption of the leader caused by the dither motion we can employ the simultaneous perturbation stochastic approximation method [18], which reduces the number of dither directions and measurements required for the gradient approximation.

Currently, gradient climbing methods for formations of underactuated vehicles, and robust redesigns that address the effect of the external disturbances such as wind and flow are being developed. We will further study dynamic field distributions for tracking a slowly varying/moving maxima which is an important problem in practice.

#### REFERENCES

- [1] N.E. Leonard and E. Fiorelli. Virtual leaders, artificial potentials and coordinated control of groups. In *Proceedings of the 40th IEEE Conference on Decision and Control*, pages 2968–2973, Orlando, Florida, 2001.
- [2] P. Ögren, E. Fiorelli, and N.E. Leonard. Cooperative control of mobile sensor networks: Adaptive gradient climbing in a distributed network. *IEEE Transactions on Automatic Control*, 49(8):1292–1302, 2004.
- [3] V. Gazi and K.M. Passino. Stability analysis of social foraging swarms. *IEEE Transactions on Systems, Man, and Cybernetics*, 34(1):539–557, 2004.
- [4] M. Arcak. Passivity as a design tool for group coordination. To appear in *IEEE Transactions on Automatic Control*, 2007.
- [5] H. Bai, M. Arcak, and J.T. Wen. Group coordination when the reference velocity is available only to the leader: an adaptive design. To appear in *Proceedings of 2007 American Control Conference*. New York City, NY, 2007.
- [6] C. Zhang, A. Siranosian, and M. Krstić. Extremum seeking for moderately unstable systems and for autonomous target tracking without position measurements. In *Proceedings of the American Control Conference*, Minneapolis, MN, 2006.
- [7] C. Zhang, D. Arnold, N. Ghods, A. Siranosian, and M. Krstić. Source seeking with nonholonomic unicycle without position measurement—part I: Tuning of forward velocity. In *Proceedings of the 45th IEEE Conference on Decision and Control*, pages 3040–3045, San Diego, CA, 2006.
- [8] R. Bachmayer and N.E. Leonard. Vehicle networks for gradient descent in a sampled environment. In *Proceedings of the 41st IEEE Conference on Decision and Control*, pages 113–117, Las Vegas, NV, 2002.
- [9] J. Cortés, S. Martínez, T. Karatas, and F. Bullo. Coverage control for mobile sensing networks. *IEEE Transactions on Robotics and Automation*, 20(2):243–255, 2004.
- [10] T. Huntsberger, P. Pirjanian, A. Trebi-Ollennu, H. D. Nayar, H. Agazarian, A. J. Ganino, M. Garrett, S. S. Joshi, and P. S. Schenker. Campout: A control architecture for tightly coupled coordination of multirobot systems for planetary surface exploration. *IEEE Transactions on Systems, Man, and Cybernetics-Part A: Systems and Humans*, 33(5):550–559, 2003.
- [11] K.M. Passino. Biomimicry of bacterial foraging for distributed optimization and control. *IEEE Control Systems Magazine*, 22(3):52–67, 2002.
- [12] L. R. Shugart, J. F. McCarthy, and R. S. Halbrook. Biological markers of environmental and ecological contamination: An overview. *Risk Analysis*, 12(3):353–360, 1992.
- [13] K.B. Ariyur and M. Krstić. *Real-Time Optimization by Extremum-Seeking Feedback*. Wiley-Interscience, Hoboken, NJ, 2003.
- [14] A.R. Teel and D. Popović. Solving smooth and nonsmooth multivariable extremum seeking problems by the methods of nonlinear programming. In *Proceedings of the 2001 American Control Conference*, pages 2394–2399, Arlington, VA, 2001.
- [15] D.F. Chichka, J. Speyer, and C.G. Park. Peak seeking control with application to formation flight. In *Proceedings of the 38th IEEE Conference on Decision and Control*, Phoenix, AZ, 1999.
- [16] P. Binetti, K. B. Ariyur, M. Krstić, and F. Bernelli. Control of formation flight via extremum seeking. In *Proceedings of the 2002 American Control Conference*, Anchorage, AK, 2002.
- [17] J. Nocedal and S.J. Wright. *Numerical Optimization*. Springer-Verlag, New York, 1999.
- [18] J.C. Spall. Multivariable stochastic approximation using a simultaneous perturbation gradient approximation. *IEEE Transactions on Automatic Control*, 37(3):332–341, 1992.
- [19] J.C. Spall. Adaptive stochastic approximation by the simultaneous perturbation method. *IEEE Transactions on Automatic Control*, 45(10):1839–1853, 2000.
- [20] C. Zhang and R. Ordóñez. Numerical optimization-based extremum seeking control of LTI systems. In *Proceedings of the 44th IEEE Conference on Decision and Control*, Sevilla, Spain, MN, 2006.
- [21] C. Zhang and R. Ordóñez. Extremum seeking control based on numerical optimization and state regulation—part I: Theory and framework. In *Proceedings of the 45th IEEE Conference on Decision and Control*, pages 4466–4471, San Diego, CA, 2006.
- [22] N. Biggs. *Algebraic Graph Theory*. Cambridge University Press, second edition, 1993.
- [23] H. K. Khalil. *Nonlinear Systems*. Prentice Hall, Upper Saddle River, NJ, third edition, 1997.
- [24] J.E. Dennis and R.B. Schnabel. *Numerical Methods for Unconstrained Optimization and Nonlinear Equations*. SIAM, Philadelphia, 1996.
- [25] J. Kiefer and J. Wolfowitz. Stochastic estimation of a regression function. *Annals of Mathematical Statistics*, 23:462–466, 1952.
- [26] J.R. Blum. Multidimensional stochastic approximation methods. *Annals of Mathematical Statistics*, 25:737–744, 1954.